Condensed Matter Science

Geometric Structure

Determination of formal oxidation state of Co in MBE-grown co-doped TiO_2(001) anatase epitaxial films by x-ray absorption spectroscopy
Chambers, S.A., T. Droubay, S. Thevuthasan, N.H. Hamdan

Fs x-ray measurement of short-range structural dynamics in VO_2 during a photo-induced phase transition
Cavalleri, A., H.W. Chong, T.E. Glover, R.W. Schoenlein, C.V. Shank

Highly sensitive XAS with single x-ray pulses at 1 kHz
Bressler, C., M. Saes, M. Chergui, R. Abela, D. Grolimund, P.A. Heimann, R.W. Schoenlein, S.L. Johnson, A.M. Lindenberg, R.W. Falcone

Light induced intersystem crossing in $Fe[(py)_3tren](PF_6)_2$ crystals
Chong, H.W., A. Cavalleri, T.E. Glover, R.W. Schoenlein, C.V. Shank

Resonant x-ray fluorescence holography: Three-dimensional atomic imaging in true color
Omori, S., L. Zhao, S. Marchesini, M. A. Van Hove, C. S. Fadley

Ultrafast measurements of liquid carbon and liquid silicon
Johnson, S., A. Lindenberg, A. MacPhee, P.A. Heimann, R.W. Falcone

Determination of Formal Oxidation State of Co in MBE-Grown Co-doped TiO_2(001) Anatase Epitaxial Films by X-ray Absorption Spectroscopy

S.A. Chambers[1], T. Droubay[1], S. Thevuthasan[1], N.H. Hamdan[2]
[1]Fundamental Science Division, Pacific Northwest National Laboratory
Richland, WA 99352, U.S.A.
[2]Lawrence Berkeley National Laboratory, Berkeley, CA 94720, U.S.A.

INTRODUCTION

Diluted magnetic semiconductors (DMS) consist of nonmagnetic semiconducting materials doped with a few atomic percent of impurity magnetic cations. Magnetic coupling occurs by virtue of exchange interactions between the magnetic spins and free carriers in the semiconductor. The interaction can occur via *p-d* or *d-d* exchange, and can lead to antiferromagnetic or ferromagnetic coupling, depending on the concentration and the local structural environment of the magnetic impurity. DMS materials grown as thin epitaxial films can be used as spin injectors for semiconductor heterostructures, provided they are ferromagnetic.

Virtually all conventional DMS materials exhibit Curie temperatures of ~100K or less and must be *p*-type, which means that the exchange interaction leading to ferromagnetic behavior is hole mediated. Most of the effort expended to date on understanding the crystal growth and properties of thin-film DMS materials has focused on Mn-doped II-VI, III-V, and Group IV semiconductors.[1-4] Relatively little effort has gone into the investigation of "nontraditional" semiconductors, such as semiconducting oxides, to see if they are more robust magnetically. However, one such oxide - Co-doped TiO_2 anatase ($Co_xTi_{1-x}O_2$) - has recently been discovered to be the most magnetically robust DMS with regard to magnetic moment at saturation, coercivity, remanence, and Curie temperature.[5] Indeed, it is one of the very few DMS materials demonstrated to exhibit ferromagnetic behavior above 300K. In addition, it has been shown that the material can be grown epitaxially by both pulsed laser deposition (PLD)[6] and oxygen plasma assisted molecular beam epitaxy (OPA-MBE)[5] on $SrTiO_3$(001) and $LaAlO_3$(001). However, the resulting magnetic properties differed considerably for the two growth methods, with significantly better properties exhibited by OPA-MBE grown material.

In order to understand the mechanism of magnetism in this fascinating material, it is essential to know the charge state of the magnetic cation (Co), and the doping type. We have utilized Co L-edge x-ray absorption spectroscopy (XAS) at beamline 9.3.2 to determine the Co charge state.

EXPERIMENT

Epitaxial $Co_xTi_{1-x}O_{2-x}$ films of high structural quality were grown by OPA-MBE on $LaAlO_3$(001)[7] using a system at PNNL described in detail elsewhere.[8] The resulting samples were then transferred through air to beamline 9.3.2 and XAS measurements were made in total electron yield mode at the Co L-edge, Ti L-edge, and O K-edge. X-ray absorption near-edge spectra (XANES) were also recorded for several Co standards for comparison purposes. No surface cleaning was done, as the distribution of Co has been shown to be strongly modified by post-growth annealing at the temperatures required to rid the surface of carbon, or remove sputter damage.

RESULTS

We show in Fig. 1 Co L-edge XAS data for three films with different Co mole fractions (x) (Fig. 1a-c), and for standards containing Co in different oxidation states and local structural environments (Fig. 1d-g). The $CoTiO_3$ standard was a powder, CoO was a (001)-oriented bulk single crystal, γ-Co_2O_3 was a 100 nm thick (001)-oriented epitaxial film grown on MgO(001) at PNNL, and the Co metal standard was a polycrystalline film evaporated *in situ* in the XAS chamber. Comparison of all film spectra with those for the standards reveals a good fit with both $CoTiO_3$ and CoO, which both contain Co^{+2}, but a very poor fit for both γ-Co_2O_3, which contains Co^{+3}, and for Co metal. The fit to $CoTiO_3$ is better than that to CoO. However, there is some similarity between the reference spectra for CoO and γ-Co_2O_3, particularly in the vicinity of the feature at 784 eV. This result indicates that there may be some Co^{+3} in the CoO single crystal. The very high degree of similarity between the spectra for the Co-doped anatase films and the $CoTiO_3$ standard establishes that Co in the former is in the +2 formal oxidation state. Interestingly, using the Co evaporation rate and oxygen plasma beam intensity we have used for the growth of $Co_xTi_{1-x}O_{2-x}$ result in the epitaxial growth of metastable γ-Co_2O_3 on MgO(001). Therefore, the anatase lattice stabilizes the formation of Co(II), even though the conditions would result in Co(III) formation if pure Co oxide were allowed to grow under comparable

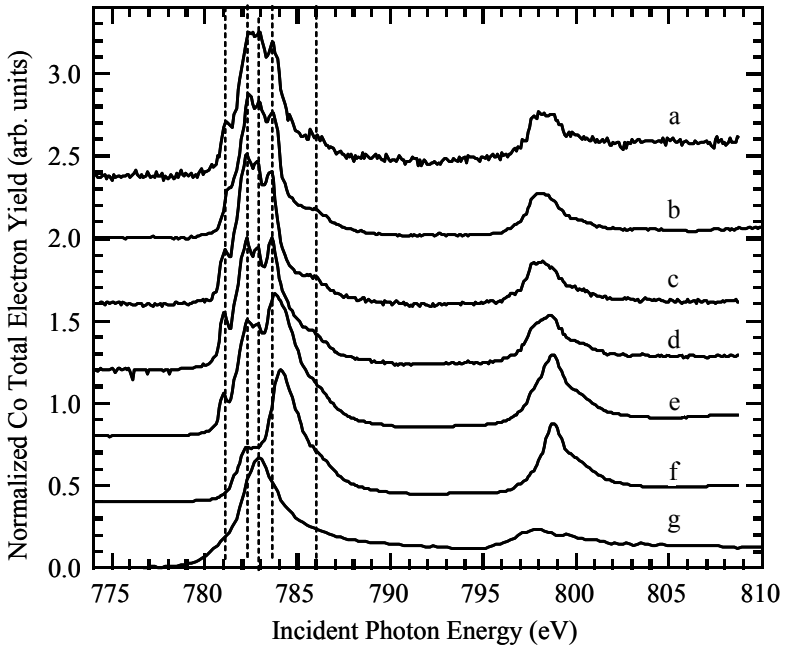

conditions.

Fig. 1 Co L-edge XAS for 20 nm thick films of epitaxial $Co_xTi_{1-x}O_{2-x}$ on $LaAlO_3$(001): (a) x = 0.01, (b) x = 0.06, (c) x = 0.08. Also shown are spectra for reference compounds containing Co in different formal oxidation states: (d) $CoTiO_3$, (e) CoO, (f) γ-Co_2O_3, and (g) Co metal.

SIGNIFICANCE

Ion channeling measurements conducted at PNNL reveals that Co substitutes for Ti in the anatase lattice. Furthermore, Hall effect measurements carried out at PNNL show that these films are *n*-type semiconductors as grown, despite the fact that no intentional *n*-type doping was carried out. The origin of the *n*-type doping may have to do with the presence of H in the film,

which has been detected by ^{19}F nuclear reaction analysis at PNNL at a concentration that is of the same order of magnitude as that of the free carriers – 10^{19} to 10^{20} cm^{-3}. H may be the direct dopant, as occurs in *n*-ZnO.[9] Alternatively, H_2, which is present in the growth chamber at a very low partial pressure, may partially reduce lattice oxygen during growth to produce OH and a free donor electron according to the reaction $O^{-2}_{(lattice)} + (1/2)H_2 \rightarrow OH^-_{(lattice)} + e^-$. This phenomenon is currently under more detailed investigation.

It thus appears that Co-doped anatase TiO_2 is ferromagnetic by virtue of *electron* mediated exchange interaction between Co^{+2} cations that substitute for Ti^{+4} in the lattice. In order to maintain charge neutrality, each substitutional Co^{+2} must be accompanied by an O^{-2} vacancy. However, such vacancies are uncharged and therefore do not contribute any donor electrons. In fact, *n*-type semiconducting behavior and Co substitution are independent phenomena; some highly resistive films are nonmagnetic despite having several at. % Co. Indeed, the magnetization depends as much on the free carrier concentration as on the presence of substitutional Co, as expected for a DMS.

Significantly, virtually all other known DMS materials are ferromagnetic by virtue of *hole* mediated exchange interaction, which has been thought to be the stronger interaction.[10] Therefore, Co-doped TiO_2 anatase is a highly unusual and potentially very important DMS in that it exhibits strong electron mediated exchange interaction at temperatures of at least 500K. No other known DMS exhibits these properties.

REFERENCES

1. R. Fiederling, M. Keim, G. Reuscher, W. Ossau, G. Schmidt, A. Waag, L.W. Molenkamp, Nature **402**, 787 (1999).
2. B.T. Jonker, Y.D. Park, B.R. Bennett, H.D. Cheong, G. Kioseoglou, A. Petrou, Phys. Rev. **B62**, 8180 (2000).
3. R.K. Kawakami, Y. Kato, M. Hanson, I. Malajovich, J.M. Stephens, E. Johnston-Halperin, G. Salis, A.C. Gossard, D.D. Awschalom, Science **294**, 131 (2001).
4. Y.D. Park, A.T. Hanbicki, S.C. Irwin, C.S. Hellberg, J.M. Sullivan, J.E. Mattson, T.F. Ambrose, A. Wilson, G. Spanos, B.T. Jonker, Science **295**, 651 (2002).
5. S.A. Chambers, S. Thevuthasan, R.F.C. Farrow, R.F. Marks, J.-U. Thiele, L. Folks, M.G. Samant, A.J. Kellock, N. Ruzycki, D.L. Ederer, U. Diebold, Appl. Phys. Lett. **79**, 3467 (2001), and, S.A. Chambers, Mat. Today, to appear, April issue (2002).
6. Y. Matsumoto, M. Murakami, T. Shono, T. Hasegawa, T. Fukumura, M. Kawasaki, P, Ahmet, T. Chikyow, S.-Y. Koshihara, H. Koinuma, Science **291**, 854 (2001).
7. S.A. Chambers, C. Wang, S. Thevuthasan, T. Droubay, D.E. McCready, A.S. Lea, V. Shutthanandan, C.F. Windisch, Jr., submitted to Thin Solid Films (2002).
8. S.A. Chambers, Surf. Sci. Rep. **39**, 105 (2000).
9. D.M. Hofman, A. Hofstaetter, F. Lieter, H. Zhou, F. Henecker, B.K. Meyer, S.B. Orlinskii, J. Schmidt, and P.G. Baranov, Phys. Rev. Lett. **88**, 045504-1 (2002).
10. T. Dietl, H. Ohno, F. Matsukura, J. Cibert and D. Ferrand, Science **287**, 1019 (2000).

The work was funded by a Laboratory Directed Research and Development grant associated with the PNNL Nanoscience and Technology Initiative, and by DOE BES Materials Science.

Principal Investigator – S.A. Chambers. Phone – (509) 376-1766. E-mail – sa.chambers@pnl.gov

Fs x-ray measurement of short-range structural dynamics in VO_2 during a photo-induced phase transition.

A. Cavalleri[1], H.W.Chong[1],T.E. Glover[2], R.W. Schoenlein[1], and C.V. Shank[1]
[1]Materials Sciences Division
[2]Advanced Light Source Division
Ernest Orlando Lawrence Berkeley National Laboratory,
University of California, Berkeley, California 94720, USA

INTRODUCTION

The main goal of this experiment is the measurement of femtosecond structural and electronic dynamics during a phase transition in the correlated, non-magnetic oxide VO_2. This material undergoes a metal-insulator transition at 340 K, accompanied by a structural transformation between a low-T monoclinic and a high-T rutile phase. The role of electron-electron and electron-phonon correlations during this process has long been debated[1]. Current understanding favors the picture of a Mott-Hubbard insulator (low-T phase), which is turned into a simple metal upon relaxation of a structural distortion above the transition temperature.

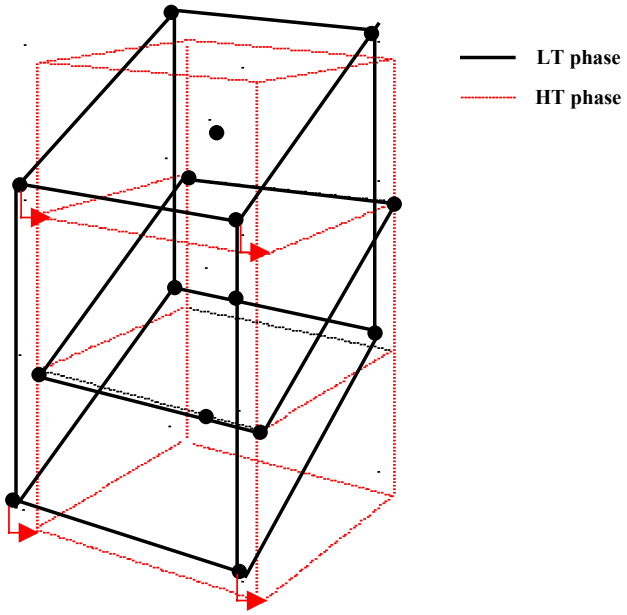

Fig. 1. Structural transition between the low-T monoclinic and high-T rutile phases of Vanadium Dioxide. A transverse optical phonon drives the transition within less than 1 picosecond.

Recent femtosecond x-ray diffraction measurements[2] have indicated that the structural transition has a very fast component, whereby long-range order between Vanadium atoms is changed within less than one picosecond. Static Raman spectra suggest that this structural transition may be impulsively induced, by photo-excitation of transverse optical phonons involving Vanadium-Vanadium distortions[3]. Further, while an additional strong V-O Raman-active mode is found (not shown in the figure) it is also known that a prominent signature of the metal insulator transition can be found near the Oxygen absorption edge[4], due to the strong hybridization of p and d orbitals from the Vanadium and Oxygen atoms, respectively.

CURRENT STATUS

The correlation between excitation of these vibrational modes and ultrafast changes in the electrical properties is the main object of our study. The experiments require combined measurement of the ultrafast electrical transition (by means of femtosecond NEXAFS spectroscopy) and of short-range structural dynamics, with sensitivity to both light (Oxygen) and heavier (Vanadium) elements (by means of femtosecond EXAFS).

The experiment will be performed using femtosecond pulses of synchrotron radiation available at the Advanced Light Source, in the spectral range between 500-800 eV, i.e. across the Vanadium L-edges and the Oxygen K-edge. The feasibility of these measurements has been demonstrated in grazing incidence geometry, where signatures of both phase transitions (electrical and structural) have been identified. For this purpose, we have performed static experiments (by varying the temperature of the sample), and time-resolved pump-probe experiments in the hundred picosecond timescale.

Because of the inconvenience of grazing incidence geometry, current efforts are dedicated to the fabrication of thin (0.05 μm), free-standing films of Vanadium Dioxide, using a combination of deposition and etching techniques. In the future, direct measurements of the EXAFS and NEXAFS component of the VO_2 transition will be conducted in a transmission geometry.

REFERENCES

1. A. Zylberstein, N. Mott *Phys. Rev. B* **11**, 4383 (1975); R.M. Wentzcovic, W.W. Schultz, P.B. Allen *Phys. Rev. Lett.* **72**, 3389 (1994).
2. A. Cavalleri et al. *Phys. Rev. Lett*. **87**, 237401 (2001).
3. Ramakant Srivastava and L.L. Chase *Phys. Rev. Lett*. 27, 727 (1971).
4. M. Abbate et al. *Phys. Rev. B*. **43**, 7263 (1991).

ACKNOWLEDGMENTS

This work was supported by the Director, Office of Energy Research, Office of Basic Energy Sciences, Materials Science Division, of the U.S. Department of Energy under Contract No. DE-AC03-76SF00098.

CONTACT

Principal investigator: Robert Schoenlein, Materials Sciences Division, Ernest Orlando Lawrence Berkeley National Laboratory. Email: rwschoenlein@lbl.gov. Telephone: 510-486-6557.

Highly sensitive XAS with Single X-Ray Pulses at 1 kHz

C. Bressler[1], M. Saes[1,2], M. Chergui[1], R. Abela[2], D. Grolimund[2], P. A. Heimann[3], R. W. Schoenlein[3], S. L. Johnson[4], A. M. Lindenberg[4], and R. W. Falcone[4]

[1]Institut de Physique de la Matière Condensée, University of Lausanne, CH-1015 Lausanne, Switzerland
[2]Swiss Light Source, Paul Scherrer Institut, CH-5232 Villigen, Switzerland
[3]Advanced Light Source, Ernest Orlando Lawrence Berkeley National Laboratory, University of California, Berkeley, California 94720, USA
[4]Department of Physics, University of California, Berkeley, California 94720, USA

INTRODUCTION

We are currently developing a scheme to exploit pulsed x-radiation for structural dynamics studies at beamline 5.3.1 via time-resolved X-ray absorption spectroscopy (XAS). While XANES is complicated to interpret from a structural point of view, it contains rather simple phenomena like the chemical shift, which describes the oxidation state of the atom. On the other hand, EXAFS delivers a detailed picture of the local environment [1], and interatomic separations can nowadays be determined with an accuracy down to 100 fm [2]. In addition, EXAFS requires no periodic structures (as required in x-ray diffraction), and can be readily applied to disordered systems, e.g., liquids.

Laser-pump SR-probe experiments depend on the available number of x-ray photons per single pulse at the repetition rate of the exciting laser, which is typically 1 kHz for commercial amplified fs-lasers. Therefore, such experiments can use only about 10^{-5} - 10^{-6} of the available photon flux at a synchrotron with its much higher pulse repetition rate of 100 - 500 MHz. We have performed calculations of the expected pump-probe signal for a given condensed phase chemical system [3,4], which also underline the general utility of time-resolved XAS in condensed phase dynamics research.

EXPERIMENTAL APPROACH

X-radiation from the ALS camshaft pulse (detected with an APD behind the sample) is singled out with a gated integrator (opening window ca. 20 ns). In order to record high-quality spectra in a pump-probe configuration we have employed the following scheme: The gated integrator is triggered at twice the laser repetition rate, so that every second x-ray pulse corresponds to the static (= unexcited) sample, while the other x-ray pulses monitor the transmission following photoexcitation at an adjustable time delay. Therefore, the gated integrator delivers an output of alternatively laser-pumped and unpumped intensities, which are then read into the computer and appropriately sorted. With this scheme we can record high-quality EXAFS spectra of the photoinduced changes. Indeed, a careful analysis of the measured noise shows that we have nearly achieved the shot noise limit in this configuration. The measured noise is considerably reduced over other methods, which include additional systematic noise sources. The step-scanning monochromator induces vibrations, which result in a rather constant noise source on the transmitted intensity. This is considerably reduced, when no optics move, and the decreasing storage ring current is observed by a corresponding broadening of the pulse height distribution. In addition, using our latest development by measuring the difference spectra *during* a monochromator scan reduces the noise even more. After correcting the statistically derived effective flux for the limited x-ray absorption in the 30 μm thick APD, our measurements are very close to the specified flux of this beamline [5].

RESULTS AND DISCUSSION

With our new difference-signal detection scheme we make best use of the x-ray source, since the recorded noise on these spectra correspond nearly entirely to the expected shot noise limit. But we can also record high-quality EXAFS without employing the difference measurement technique. Figure 1 illustrates this for the case of aqueous iodide. The energy spectrum has already been transformed into k-space (Fig. 1a), but the original data has not been treated (e.g., smoothed or Fourier-filtered). This spectrum represents a single scan accumulating 2500 single x-ray pulses per data point. The fit (and its Fourier transform, Fig. 1b) delivers a nice agreement with the literature, and the accuracy for determining the nearest neighbor shell of oxygen atoms is better than 10 pm [4].

Fig. 1 also illustrates the potential for measuring the nearest-neighbor distance in photogenerated iodine radicals. The I-O distance should change considerably upon photodetachment. Values for iodine are currently unknown, but in a theoretical study of aqueous Br radicals the predicted Br-O distance changed from 335 pm for the ion to ca. 280 pm for the neutral radical [6]. Assuming a similar reduction in the iodine-oxygen distances would result in a pronounced change in the EXAFS signal, as shown in the dashed curves in Fig. 1.

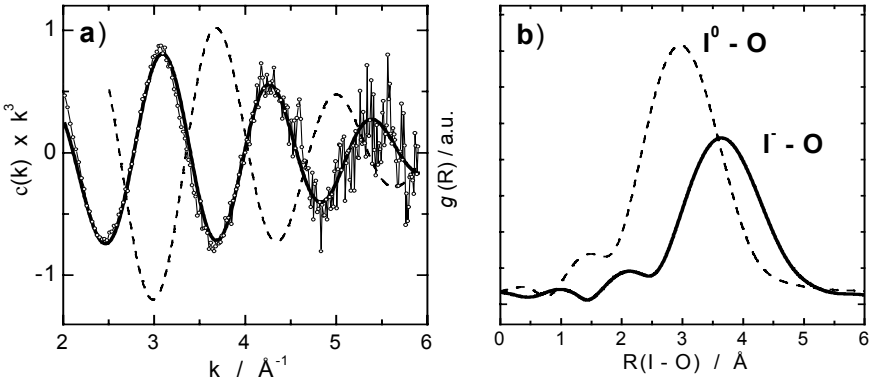

Figure 1. Static EXAFS above the L_3 edge of iodine of aqueous iodide (NaI concentration: 0.7 mol/l, thickness: 0.1 mm). Original data (open circles), and their fit (solid line) is shown in a), and the Fourier transform showing the nearest neighbor I-O distance in b) (solid line). For comparison, a simulation of the expected EXAFS of atomic iodine is shown (dashed curve in a) together with its Fourier transform (dashed curve in b).

Exploiting our difference measurement technique we have attempted to measure the photo-induced chemical shift due to UV photoionization of the central Fe atom in aqueous $[Fe^{II}(CN)_6]^{4-}$ with a synchronized fs laser. The chemical shift of ca. 1 eV around the Fe K edge was observed in static samples containing either $[Fe^{II}(CN)_6]^{4-}$ or $[Fe^{III}(CN)_6]^{3-}$ (concentration 0.2 mol/l, sample thickness 0.1 mm), as illustrated in Fig. 2 a) and b). Then we excited a liquid jet with the reactant species $[Fe^{II}(CN)_6]^{4-}$ only with 100 μJ of 266 nm light, and recorded the transient changes. Due to the low excitation yield of below 0.4 % we could not observe the chemical shift on the 100 ps time scale (Fig. 2 c) and d). However, with improved statistics exploiting the first 100 ns of the multibunch train following photoexcitation we did observe a photoinduced change in the XAS. In Fig. 3 a) the average of 20 spectra are shown for each the unpumped and the pumped sample (offset for clarity). Fig. 3 b) shows the difference signal of Fig. 3 a) together with a simulation assuming laser-induced evaporation of ca. 100 nm of the 0.1 mm thick sample. While this nicely reproduces the majority of the measured difference spectrum, we still observe some discrepancy around the 1s → 4p pre edge feature, as shown in the residual spoectrum in Fig. 3 c). The double minimum shape of decreased transmission (clearly visible in the smoothed spectrum) indicates a

broadening of this feature, which has been observed in temperature-dependent XANES studies. The elevated temperature of the laser-heated sample could account for this observation.
While our current sensitivity does not allow to unambiguously observe the chemical shift for less than 0.4 % excited species, current improvements on the laser excitation process will permit us to boost the product yield into the 1-5 % range.

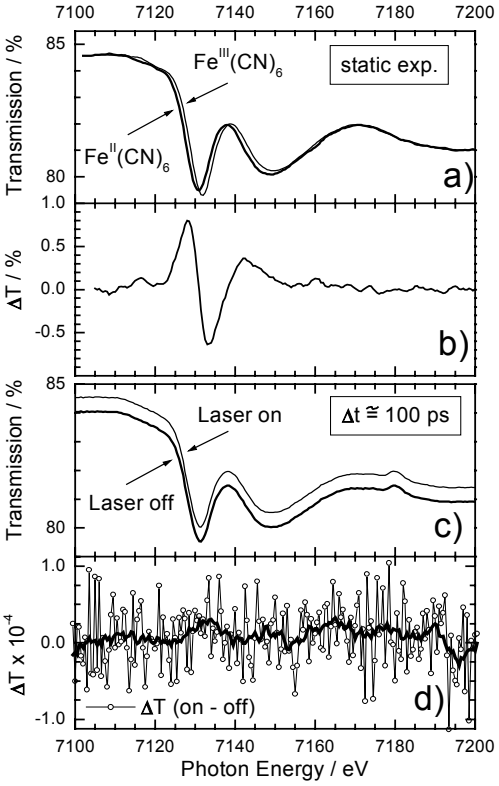

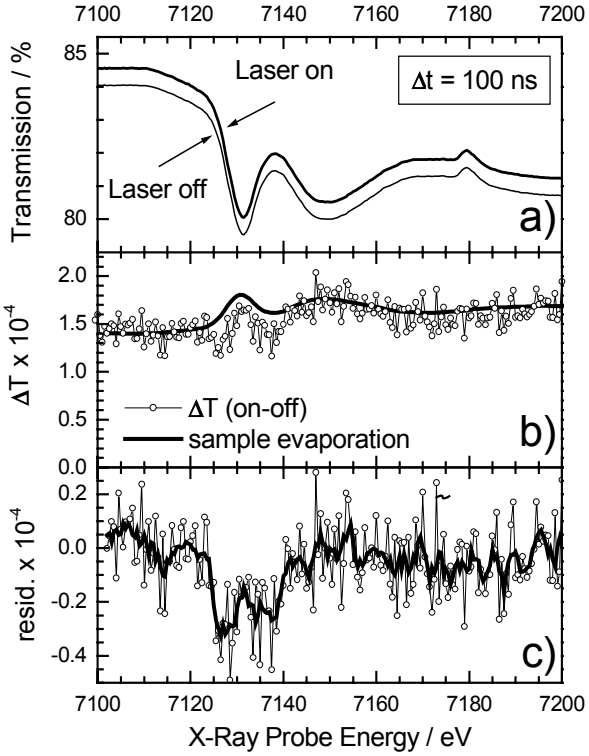

REFERENCES

1. E. A. Stern, S. M. Heald, in: *Handbook on Synchrotron Radiation*, Vol. 1B, Ed: E. E. Koch, North Holland (1983), pp. 955 fff; B. K. Agarwal, *X-Ray Spectroscopy*, Springer (1991)
2. U. Buontempo, A. Filipponi, P. Postorino, R. Zaccari, J. Chem. Phys. **108**, 4131 (1998)
3. C. Bressler, M. Saes, M. Chergui, P. Pattison, R. Abela, Nucl. Instrum. Meth. **A 467-468**, 1444 (2001)
4. C. Bressler, M. Saes, M. Chergui, D. Grolimund, R. Abela, P. Pattison, J. Chem. Phys. (in press, 2002)
5. C. Bressler, M. Saes, M. Chergui, D. Grolimund, R. Abela, to appear in: *Femtochemistry and Femtobiology*, ed. A. Douhal, World Scientific (2002)
6. M. Roeselova, U. Kaldor, P. Jungwirth, J. Phys. Chem. A104, 6523 (2000)

This work was supported by the Swiss National Science Foundation (SNF) via contract no. FN 20-59146.99, the Paul Scherrer Institut and the Advanced Light Source.

Principal investigator: Christian Bressler, Institute of Condensed Matter Physics, University of Lausanne, CH-1015 Lausanne, Switzerland. Email: Christian.Bressler@ipmc.unil.ch. Telephone: ++41-21-692-3676.

Light Induced Intersystem Crossing in $Fe[(py)_3tren](PF_6)_2$ Crystals

H.W.Chong[1] ,A. Cavalleri[1],T.E. Glover[2], R.W. Schoenlein[1], and C.V. Shank[1]
[1]Materials Sciences Division
[2]Advanced Light Source Division
Ernest Orlando Lawrence Berkeley National Laboratory,
University of California, Berkeley, California 94720, USA

INTRODUCTION

$Fe[(py)_3tren]^{2+}$ is a member of a class of octehedrally coordinated iron-based transition metal complexes which undergoes an $\Delta S=2$ spin-crossover transition upon light excitation. This transition proceeds first by electronic excitation from a low-spin singlet ground state to a metal-to-ligand charge transfer state, followed by subsequent relaxation to a high-spin quintuplet state, a process completed within roughly 500 femtoseconds at room temperature. The lifetime of the excited, high-spin state is roughly 700 picoseconds at room temperture, after which the system relaxes back to the singlet ground state. Concomitant with this highly spin-forbidden electronic transition is a structural dilation of the ligand cage surrounding the iron. Current experimental work has only been able to establish a symmetric dilation of the ligand cage in the high-spin state, with the bonds of the first shell of octehedrally-coordinated nitrogen distended by 10% relative to the low-spin state. It has been conjectured, however, that in the intermediary stages of the spin-crossover process, the ligand cage, in fact, distorts asymmetrically, and that it is this distortion which gives energetic preference to the high-spin state. With the ultrashort x-ray pulse capabilities of beamline 5.3.1, we hope to observe dynamically these structural changes in the iron's ligand cage to provide evidence of the role, if any, of the structural changes in the spin-crossover behavior of $Fe[(py)_3tren]^{2+}$.

CURRENT STATUS

We intend to analyze EXAFS and near-edge structures of the iron and nitrogen to determine the atomic motion of the ligand cage as the system evolves after excitation. Due to the signal-limited nature of this experiment, a great deal of effort has gone into the design and characterization of the measurement apparatus. Offline, work has focused on crystal synthesis and sample preparation to provide for optimal signal-to-noise, and optical characterization of the dynamics to determine optimal excitation conditions.

Static spectra of the iron K-edge have been recorded for the candidate molecule and a chemically synthesized high-spin analogue to anticipate the potential spectral changes that may be observed between the two states. These time-independent spectra are shown in Fig. 1 and clearly demonstrate a near-edge shift between the high and low spin states. We intend to next observe similar spectral shifts in a time-resolved fashion following excitation by femtosecond laser pulses.

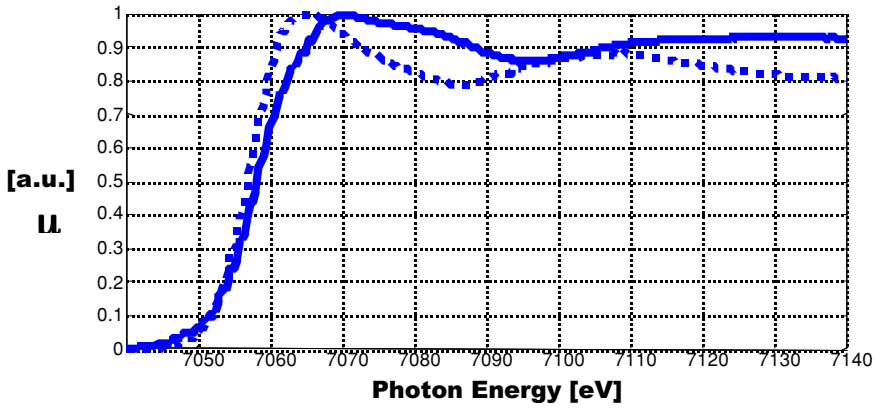

Figure. 1 Static EXAFS spectra of high (dashed line) and low (solid line) spin states of $Fe[(py)_3tren]^{2+}$.

ACKNOWLEDGMENTS

This work was supported by the Director, Office of Energy Research, Office of Basic Energy Sciences, Materials Science Division, of the U.S. Department of Energy under Contract No. DE-AC03-76SF00098.

CONTACT

Principal investigator: Robert Schoenlein, Materials Sciences Division, Ernest Orlando Lawrence Berkeley National Laboratory. Email: rwschoenlein@lbl.gov. Telephone: 510-486-6557.

Resonant X-ray Fluorescence Holography: Three-Dimensional Atomic Imaging in True Color

S. Omori[1,2,#], L. Zhao[1,3], S. Marchesini[1], M. A. Van Hove[1,3,4], and C. S. Fadley[1,3]

[1] Materials Sciences Division, Lawrence Berkeley National Laboratory, Berkeley, California 94720
[2] Institute of Industrial Science, University of Tokyo, Tokyo 153-8505, Japan
[3] Department of Physics, University of California, Davis, California 95616
[4] Advanced Light Source, Lawrence Berkeley National Laboratory, Berkeley, California 94720
[#]Present address: Sony Research, Kawasaki, Japan

X-ray fluorescence holography (XFH) is a relatively new experimental tool for directly determining the local three-dimensional atomic structure around a given type of atom [1-4]. This element-specific method is based on the same concept as photoelectron holography [5], but detects instead fluorescent x-ray photons.

In the first type of XFH to be demonstrated experimentally [1a], one measures the interference between the fluorescent radiation directly emitted by the excited atoms and additional wave components of the same radiation scattered by various near-neighbor atoms. It is thus necessary to measure a given fluorescent intensity as a function of the direction of emission over as large a solid angle as possible. This method, for which the fluorescent atoms inside the sample act as sources and the intensity is measured in the far field, has been termed normal x-ray fluorescence holography (XFH) [2] or more specifically "direct XFH". In parallel with the first direct XFH experiment, Gog et al. [2a] proposed and demonstrated a different approach (termed multiple energy x-ray holography (MEXH) or "inverse XFH") by applying the optical reciprocity principle and exchanging the roles of source and detector. In this case, the fluorescent atoms inside the sample become the detectors for the net field produced by the interference of the incident x-ray beam and the components of this beam that are scattered by near-neighbor atoms. With present detection systems, MEXH is faster, as the incident beam can be very intense (e.g. emitted directly from a beamline monochromator or an undulator harmonic), and one can furthermore in principle detect all of the fluorescence emitted above the sample surface. Here, one is thus measuring the total fluorescence yield of a given atomic transition as a function of the direction of the incident x-ray beam. Being able to measure at multiple energies also results in images with less aberration due to twin-image effects and other non-idealities [2,5,6]. Recent XFH/MEXH studies have demonstrated the ability to image a first-row element in the presence of a transition metal [3], and to study the local atomic environment in a quasicrystal, even though translational periodicity is lacking for such a system [4]. Current experiments are by and large detector-limited as to the speed of data acquisition. In the ALS Compendium of 2000, we have discussed a project that has successfully measured the first MEXH holograms and holographic atomic images at the ALS [7].

Even though XFH and MEXH in their current formulations offer powerful methods to probe the local atomic structure around a given atom, there still remains one deficiency: the techniques may be element-specific for the central fluorescing atom in the structure (a quality they share with extended x-ray absorption fine structure (EXAFS)), but there is no simple way to determine the

near-neighbor atomic identities. Use can be made of the differences in non-resonant x-ray scattering strengths between different atoms (as is done with differences in electron scattering strength in EXAFS), but this is only unambiguous when atomic numbers are relatively far apart, as recently illustrated for the case of O and Ni in NiO [3]. In the present work, we propose a significant improvement to MEXH, resonant x-ray fluorescence holography (RXFH), that should enable the direct discrimination of different atoms in reconstructed images, even for the most difficult cases where atomic numbers of elements involved are very close together. It is in this sense that we can finally speak of atomic images "in true color" [8].

The principle of RXFH is discussed here for the example of a binary compound of AB_3 type with close atomic numbers, specifically $FeNi_3$, for which $Z_{Ni} - Z_{Fe} = 2$ and the fractional change in atomic number is only ~0.08 [8]. The central fluorescing atom of the reconstructed images is always chosen to be atom *A* (Fe in this case), and the anomalous dispersion associated with an absorption edge for element *B* (Ni in this case) is used to selectively image atoms *B* surrounding the central atom. In the usual implementations of MEXH in which both atoms *A* and *B* are to be equally imaged, the incident x-ray energies *E* are usually chosen in such a way that they are close enough to E_{abs}^{A}, the absorption edge of element *A*, for the efficient excitation of fluorescent x-rays from *A*, but also far enough from both E_{abs}^{A} and any edges E_{abs}^{B} of atom B that the anomalous dispersion terms in the x-ray scattering factors for *A* and *B* are not significant. In RXFH, by contrast, we will choose several *E*'s in the vicinity of an absorption edge E_{abs}^{B} of element *B*. The basic idea here is thus similar to that of multiple-wavelength anomalous diffraction (MAD) for phase determinations in conventional x-ray diffraction studies, but with the significant difference that there is from the outset no phase uncertainty in MEXH.

Making use of experimentally determined x-ray scattering factors for Fe (non-resonant) and Ni (resonant), as shown in Fig. 1, we have thus theoretically simulated holograms [6b] for a large cluster of atoms representing the $FeNi_3$ lattice as the Fe Kα fluorescence at 6.4 keV is monitored while scanning through the Ni K edge at about 8.3 keV [8]. As a first trial set of data, we have finally obtained MEXH and RXFH images based on the three energies shown in Fig. 2: below, on, and above the Ni K edge. One promising procedure for imaging in RXFH is shown elsewhere [8] to be using two difference holograms for E_1-E_2 and (with reversed sign) E_3-E_2. Fig. 2 shows the $FeNi_3$ crystal structure, together with normal MEXH images and RXFH images from these difference holograms. Fig. 2 makes it clear that the Ni-atom images are strongly suppressed in the RXFH images, thus suggesting this as a new approach in x-ray fluorescence holography for identifying near-neighbor atoms to a given type of fluorescent emitter.

In conclusion, resonant x-ray fluorescence holography should make it possible to obtain additional information on near-neighbor chemical identities that would lead to a much more complete structural characterization of any system, particularly one in which possible compositional disorder on the nm scale is present, and thus to a much broader applicability for nanoscale materials characterization. Future experiments at the ALS will explore this approach experimentally.

REFERENCES

[1] (a) M. Tegze, G. Faigel, Nature 380 (1996) 49; (b) (b) G. Faigel and M. Tegze, *Rep. Prog. Phys.* **62** (1999) 355.

[2] (a) T. Gog, P.M. Len, G. Materlik, D. Bahr, C.S. Fadley, C. Sanchez-Hanke, Phys. Rev. Lett. **76** (1996) 3132; (b) P.M. Len, C.S. Fadley, and G. Materlik, in X-ray and Inner-Shell Processes: 17th International Conference, R.L. Johnson, H. Schmidt-Böcking, and B.F. Sonntag, Eds., AIP Conference Proceedings, No. 389 (AIP, New York, 1997) p. 295.
[3] M. Tegze, G. Faigel, S. Marchesini, M. Belakhovsky, O. Ulrich, Nature 407, (2000) 38.
[4] S. Marchesini, et al., Phys. Rev. Lett. 85, (2000), 4723-6
[5] G.R. Harp, D.K. Saldin, B.P. Tonner, Phys. Rev. Lett. 65 (1990) 1012; plus more recent work at the ALS by P.M. Len et al. Phys. Rev. B **59** (1999) 5857
[6] (a) P.M Len, Ph.D. thesis, University of California at Davis (1997) and (b) simulation and imaging software described at http://electron.lbl.gov/holopack/holopack.html.
[7] S. Marchesini, L.Zhao, L. Fabris, M. W. West, J. Bucher, D. K. Shuh, W. C. Stolte, M. J. Press , A.S. Schlachter, Z. Hussain, and C. S. Fadley, ALS Compendium of Abstracts 2000: http://alspubs.lbl.gov/AbstractManager/uploads/00135.pdf.
[8] S. Omori, L. Zhao, S. Marchesini, M.A. Van Hove, and C.S. Fadley, Phys. Rev. B **65** (2002) 014106.

This work was supported by the U.S. Department of Energy, Office of Science, Office of Basic Energy Sciences, Materials Sciences Division, under Contract No. DE-AC03-76SF00098..

Principal investigator: Stefano Marchesini, Materials Sciences Division, Lawrence Berkeley National Laboratory. Email: marchesini@lbl.gov. Telephone: 510-486-4581.

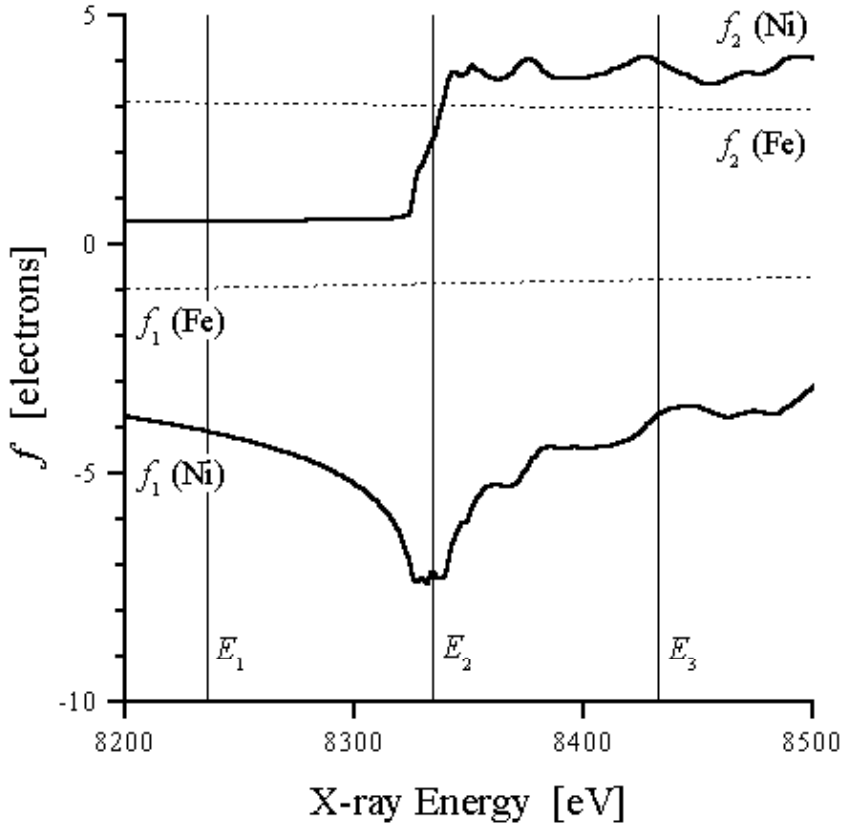

Fig. 1-- The atomic x-ray scattering factors f_1 and f_2 for Fe (dotted lines) and Ni (solid lines) as a function of x-ray energy around the *K* edge of Ni. The overall scattering factor is given by $f_{Atom} = f_0(\theta) + f_1 - if_2$, with $f_0(\theta)$ the form factor. The three energies used for the simulations of E_1, E_2 and E_3 are indicated by vertical solid lines and correspond to 8235 eV, 8334 eV, and 8433 eV, respectively.

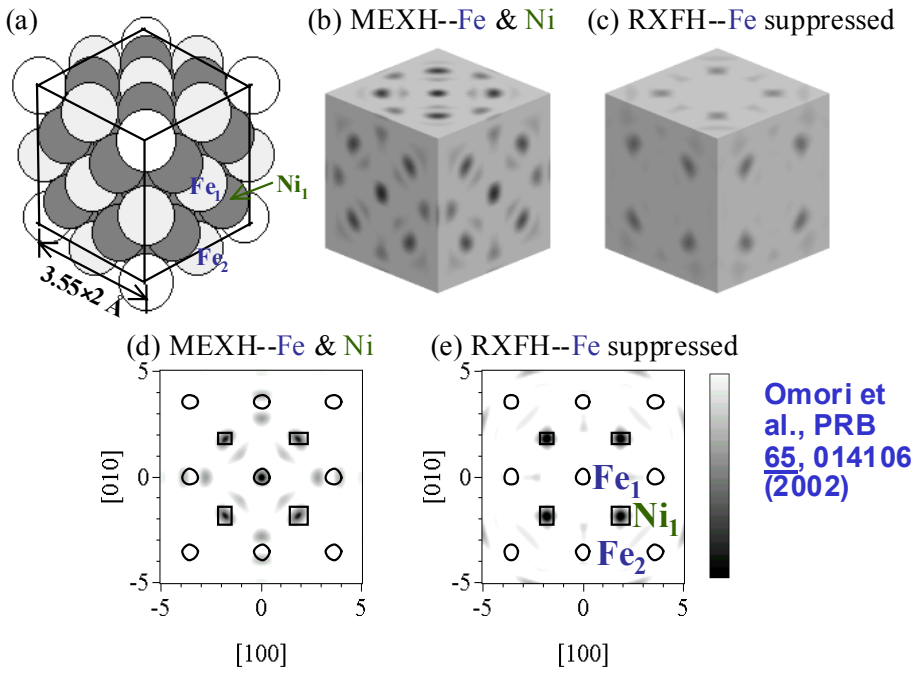

Fig. 2-- Comparison of multi-energy inverse x-ray fluorescence holographic images based on the negative of the real part of images generated using both the standard inversion algorithm (MEXH) and resonant holography (RXFH) based on two difference images (E_1-E_2 and E_3-E_2). These images are based on single-scattering cluster simulations of holograms [6b] at the three energies E_1, E_2 and E_3 for an $FeNi_3$ crystal containing about 10,000 atoms. (a) Near-neighbor atomic model of $FeNi_3$ for comparison to the reconstructed images in (b) and (c) and including 8 unit cells with the lattice constant of 3.55 Å. Fe atoms are lighter gray, and Ni atoms darker gray. The unique types of Fe and Ni atoms observed in (b) are labelled as Fe_1, Fe_2 and Ni_1. (b) Three dimensional reconstructed image from MEXH in cross section along six {001} planes. (c) Corresponding image from RXFH. The fluorescing Fe atom is located at the centers of the cubes in (a), (b) and (c). (d) Enlarged reconstructed image from MEXH in the (001) plane. (e) Corresponding enlarged image from RXFH. The true atomic positions of Fe and Ni atoms are shown as circles and squares, respectively, and certain key atomic positions are also labelled.

Ultrafast Measurements of Liquid Carbon and Liquid Silicon

S.Johnson[1] ,A. Lindenberg[1],A. MacPhee[1], P.A. Heimann[2], and R.W. Falcone[1]
[1]Department of Physics
University of California, Berkeley, California 94720, USA
[2]Advanced Light Source Division
Ernest Orlando Lawrence Berkeley National Laboratory,
University of California, Berkeley, California 94720, USA

INTRODUCTION

Conventional techniques of x-ray absorption spectroscopy, while extremely useful for studying the electronic and atomic structures of many materials, are generally not suitable for high temperature, volatile materials. The introduction of time resolution overcomes much of this difficulty: by melting thin foils with an ultrafast laser pulse and measuring the transmission of x-rays before break-up of the liquid, we can obtain useful absorption spectra of high-temperature liquids.

EXPERIMENT AND RESULTS

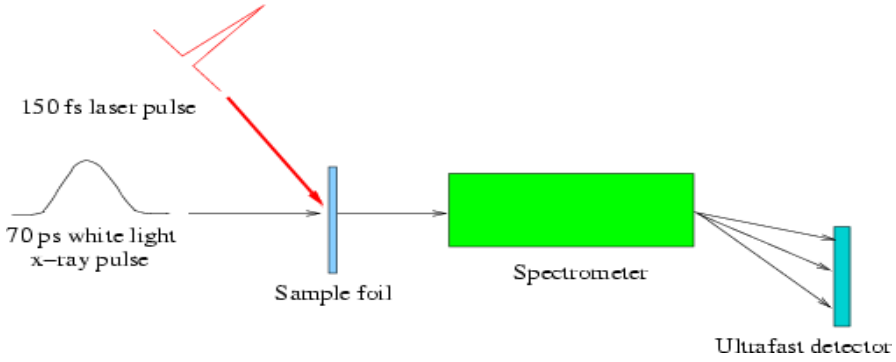

Figure 1. Sketch of experimental setup for time-resolved absorption.

Figure 1 shows a sketch of the experimental setup at beamline 5.3.1 of the Advanced Light Source. After heating the foil with an 800 nm, 150 femtosecond laser pulse, a 70 ps pulse of broad spectrum x-rays from a synchrotron bend magnet pass through the laser-excited region of the foil. A spectrometer then disperses the x-rays onto a detector. The detector is either a set of microchannel plates (for pump-probe measurements with 70 ps time resolution) or an ultrafast x-ray streak camera (for a resolution of up to 1 ps).

Figure 2 compares the *L*-edge spectrum of an unheated silicon foil with the spectrum of the foil 100 ps after laser excitation. The transition from solid to liquid results in a number of changes to the spectrum: a 50% drop and 2 eV broadening in the $L_{II,III}$ edge at 100 eV, a -1.6 ± 0.2 eV shift in the L_I edge at 150 eV, and a dramatic decrease in the magnitude of EXAFS oscillations. Model calculations based on molecular dynamics simulations of liquid silicon compare favorably with these results.

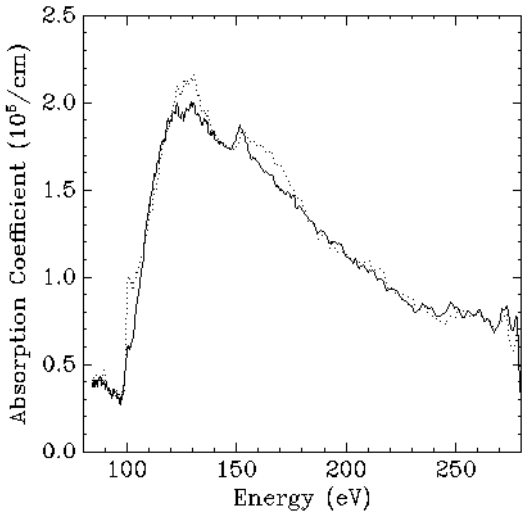

Figure 2. Absorption Spectra of silicon L-edges. Dotted line: unheated silicon; Solid line: heated silicon, 100 ps after laser.

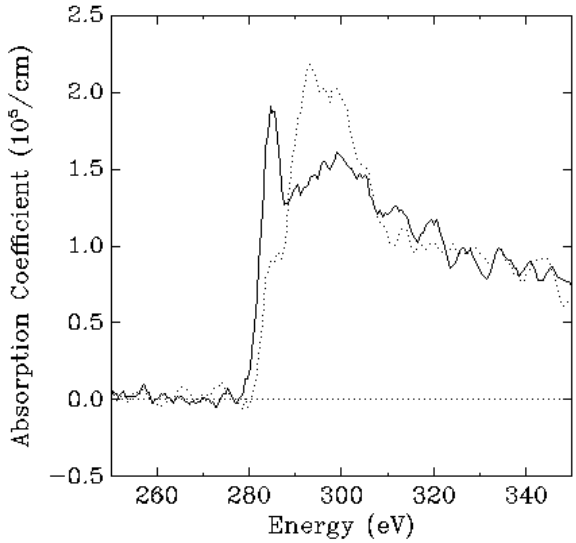

Figure 3. Carbon K-edge absorption spectra. Dotted line: unheated carbon; solid line: heated carbon, 100 ps after laser.

Measurements on foils of soft amorphous carbon, summarized in figure 3, show large differences between the unheated and heated spectra of the carbon *K*-edge. After 100 ps, the laser-induced melting causes an increase in the size of the π^* resonance at 285 eV accompanied by a decrease and 4 eV shift in the σ^* resonance at 296 eV. These changes indicate a transition in bonding geometry from the predominant sp^2 bonding characteristic of soft amorphous carbon to the collection of distorted sp bonded chains recently predicted by molecular dynamics simulations for the low-density liquid phase of carbon.[1]

REFERENCES

1. Glosli and Ree, PRL **82**, 4659 (1999).

ACKNOWLEDGMENTS

This work was supported by the Director, Office of Energy Research, Office of Basic Energy Sciences of the U.S. Department of Energy under Contract No. DE-AC03-76SF00098.

CONTACT

Principal investigator: Roger Falcone, Department of Physics, Univeristy of California at Berkeley. Email: rwfalcone@socrates.berkeley.edu. Telephone: 510-642-8916.